Measurement of Velocity Profiles in Reverse-Screw Elements of a Twin-Screw Extruder

Murali Chandrasekaran and Mukund V. Karwe
Dept. of Food Science, Rutgers University, New Brunswick, NJ 08903

A laser Doppler anemometer was used to measure velocity components for the flow of a Newtonian fluid in a reversing section of a pilot-scale corotating twin-screw extruder. Measurements were made at a fixed axial position in the intermeshing (nip) region and the translational region (away from the nip). Tangential and axial velocity profiles reached a maximum in the middle of the screw channel, indicating pressure flow. Leakage flow through the gaps between screw flights and backflow toward the hopper were observed only in the nip region. No reversal of flow was detected in the translational region. Measured velocity profiles showed substantially higher shear rates in the reversing section of the screw as compared to those in the forward-conveying section.

Introduction

Extrusion is a widely used process in the food, plastics, and pharmaceutical industries. For plastics, screw extruders are used for compounding and, increasingly, for recycling (Tadmor and Klein, 1970; Tadmor and Gogos, 1979; Fenner, 1980; Rauwendaal, 1990). In the food industry, extrusion is used to make pasta, ready-to-eat breakfast cereals, half-products (pellets), snacks, and candy. It is also used to manufacture animal feed and pet food products (Harper, 1981; Mercier et al., 1989; Kokini et al., 1992). Both single- and twin-screw extruders are commonly used in the food industry, with the choice between single- and twin-screw extrusion depending upon processing requirements and economics (Harper, 1989).

Mathematical models for transport phenomena in single-screw extruders for Newtonian as well as non-Newtonian fluids are now available (Kiani et al., 1989; Karwe and Jaluria, 1990; Chiruvella et al., 1994). Modeling twin-screw extrusion is more complex than single-screw extrusion because of the complicated geometry. Using simplifying assumptions, models for transport phenomena in twin-screw extruders for synthetic polymers and bio-polymers (food) have been developed (Bigio and Zerafati, 1988; Tayeb et al., 1988a,b, 1992; Wang and White, 1989; Kulashreshtha et al., 1991; White, 1991; Sastrohartono et al., 1992, 1994; Sebastian and Rokos, 1992; van Zulichem et al., 1992). Validations of these models are made using global quantities such as pressure or temperature at the die, mass flow rate, and average residence time. Availability of local velocity data will allow a more rigorous validation of these mathematical models. In addition, accuracy of these models in predicting shear and mixing fields, and leakage flows over the screw flights and between the screw flights, needs to be determined in order to make use of them for design and optimization purposes.

Measurement of velocity distributions in extruders has been limited to simplified, single-screw extrusion systems. Eccher and Valentinotti (1958) and Mohr et al. (1961) began with streak photography on single-screw extruders equipped with a rotating transparent barrel and stationary screw. In both these cases, measurements were made at very low barrel rotation speeds—under 10 rpm, which is very low for large extruders used in practice. Subsequently, Choo et al. (1980) made more realistic measurements using a deep-channel single-screw extruder fitted with Perspex windows. They measured velocity profiles in a concentrated glucose solution (a Newtonian fluid) by taking streak photographs of tracers from two perpendicular directions simultaneously. However, their data indicated that it was relatively difficult to make measurements near the screw root due to limited optical access. Recently, McCarthy et al. (1992) measured velocity distributions in a specially designed single-screw extruder, using a noninvasive nuclear magnetic resonance (NMR) imaging technique. The motion of a magnetically marked band of carboxymethyl cellulose across the barrel diameter was monitored. Two limiting cases were studied: (1) open die and (2)

Correspondence concerning this article should be addressed to M. V. Karwe.

closed die. The results showed that fluid velocity varied linearly between the barrel and screw surface in case (1), as predicted by theory. Similarly, effects of pressure and drag flow were observed in case (2).

Karwe and Sernas (1996) introduced laser Doppler anemometry (LDA) for measuring velocity distributions in extruders. They used an LDA system to measure velocity profiles in a corotating, self-wiping twin-screw extruder fitted with a Plexiglas window. Tangential and axial velocity measurements were made using heavy corn syrup (Newtonian) in the region away from the intermeshing zone in a 28-mm-pitch double-start forward-conveying screw element. They have shown that there are a number of advantages in using the LDA system for measuring velocity profiles in extruders. The measurement technique is noninvasive, with excellent results obtained with naturally occurring particles in the heavy corn syrup. The LDA technique has a very fast response and is accurate over a wide range of velocities. Most importantly, it was demonstrated that it is feasible to obtain velocity data in a *pilot-scale* twin-screw extruder. The only modification required was Plexiglas window, the inner surface of which was machined to match the geometry of the extruder barrel.

So far, all velocity measurements have been made with forward-conveying elements. However, a combination of forward, reverse, and kneading elements is used in a typical extrusion process. The screw configuration depends upon the application. Reverse elements increase the residence time, energy input, and shear, strongly influencing product quality (Colonna et al., 1983; Fletcher et al., 1984; Della Valle et al., 1987; Yam et al., 1994). Local velocity measurements of the fluid in the channels of reverse-conveying screws have not been reported in the literature. This study reports some of the velocity measurements made in a 20-mm-pitch, reverse-conveying screw element using laser Doppler anemometry. The velocity measurements indicated that the flow profiles in a reverse element are markedly different from a forward-conveying element due to different flow mechanisms. In addition, the flow characteristics in the translational and nip regions of a reverse element were quite different from each other.

Materials and Methods

Experimental setup

The experimental setup is shown in Figure 1. Velocity measurements were made in the screw channels of a corotating self-wiping, twin-screw extruder (Model ZSK-30, Werner & Pfleiderer Corporation, Ramsey, NJ). The internal diameter of the barrel bore (D) is 30.85 mm and the L/D is 29, where L is the total length of each screw. A Plexiglas window, 35 mm (W) × 115 mm (L), with an aluminum frame was constructed and fit into the vent port of the extruder. The Plexiglas section provided optical access to the fluid flowing in the screw channels for velocity measurements. The inner geometry of the Plexiglas section was machined and polished to match the specifications of the extruder barrel. A bore gauge (Mitutoyo Corp., Tokyo, Japan) was used to ensure that deviations in barrel diameter between the steel and Plexiglas sections were minimal. The bore gauge showed that variations in barrel diameter were at most ±0.1 mm.

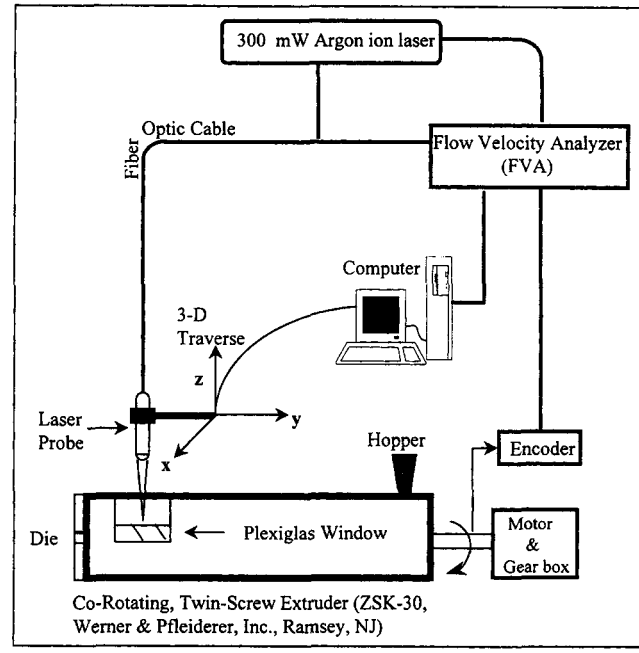

Figure 1. Experimental setup, showing the extruder and the LDA system.

Velocity measurements were performed using a four-beam 300-mW argon-ion laser Doppler anemometer system operated in the backscatter mode (Dantec Measurement Technology, Inc., Mahwa, NJ). The principles of laser Doppler anemometry have been explained by Durst et al. (1981), and its application on a extruder system by Karwe and Sernas (1996). The characteristics of the LDA used in this experimental setup are described in detail elsewhere (Karwe and Sernas, 1996). The laser beam is split into two blue beams (wavelength, $\lambda = 488$ nm) and two green beams ($\lambda = 514.5$ nm) by a beam splitter. The four-beam system measures two velocity components perpendicular to the bisector of the beams simultaneously. A Bragg cell with a frequency shift of 40 MHz was used to obtain the direction of velocity components. The beams were transmitted through a fiber-optic cable to a portable probe with a focal length of 120 mm. The fiber-optic probe picked up scattered light from particles in the flow and transmitted it to a flow-velocity analyzer (FVA). The probe was mounted on a 3-dimensional (X-Y-Z) traverse and positioned vertically above the Plexiglas window. The traverse had a spatial resolution of 0.1 mm. The traverse motion was controlled by a microcomputer, which also collected velocity data.

Experiments were performed using heavy corn syrup (Globe corn syrup, Corn Products International, Summit-Argo, IL). This is a Newtonian fluid, and is optically transparent for the laser beams to penetrate and for the scattered light to come out (Karwe and Sernas, 1996). The corn syrup has a viscosity of 74.0 Pa·s at 26.6°C and a refractive index of 1.49.

Screw elements

The screw configuration used in these experiments was assembled by using forward-conveying elements and one re-

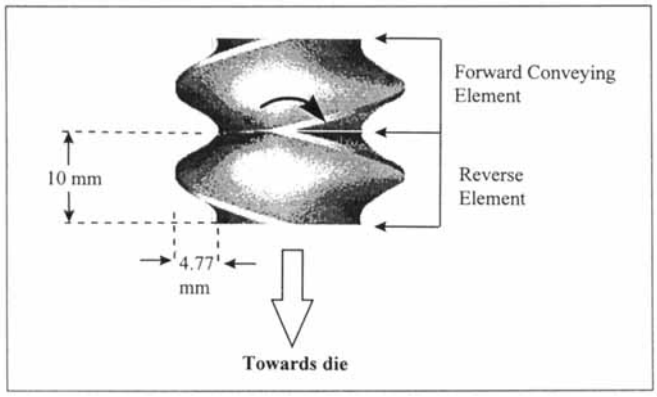

Figure 2. Screw geometry of the double-start reverse element.

The reverse element was flanked on either side by 20/10 forward-conveying elements.

verse-conveying screw element with a pitch (mm)/(length (mm) of 20/10. Details of the screw geometry are shown in Figure 2. The maximum depth for the screw channel is 4.77 mm. The equations describing the self-wiping screw profile are given in Booy (1980) and Lai-Fook et al. (1989). The reverse element was flanked on either side with 20/10-pitch forward-conveying elements (Figure 3a). Velocity data were obtained with a screw speed of 60 rpm.

A die with two holes, 5 mm long of 3 mm diameter each, was used.

Regions of measurement

Figure 3a shows the regions of velocity measurements as seen through the Plexiglas window. The intermeshing (nip) region is the region where the two screw channels meet. The translational region is the region away from the intermeshing region. The boundary between the transitional and intermeshing regions is hypothetical and perhaps cannot be identified by a single line or plane. It has been shown in the numerical studies carried out by Sastrohartono et al. (1994) that the intermeshing region does not extend a quarter turn on either side of the nip. This was found from the velocity and pressure-field contours. Also, Karwe and Sernas (1996) have shown that in the translational region considered in this article, the flow field is similar to that in the channel of a single screw. Therefore, it was assumed that the translational region was too far away from the nip to have any significant effect of the nip geometry. Figure 3a shows the tangential and axial coordinate axes in the translational region, referred to as x_T and y_T, respectively. The vertical axis, z_T, is perpendicular to the plane of the paper. Similarly, tangential, axial, and vertical coordinate axes in the nip region, x_N, y_N, and z_N, respectively, are shown in Figure 3b. In a frame of reference attached to the stationary barrel, the velocity measurements were carried out at various channel depths, that is, negative values of z_T or z_N. Measurements were made in the translational region of the right screw (screw 2 in Figure 3a) and in the nip region at a fixed axial location.

The center point of the cross in Figure 3a represents the measuring volume, that is, the intersection volume of the four beams. Figure 3b illustrates a section taken normal to the

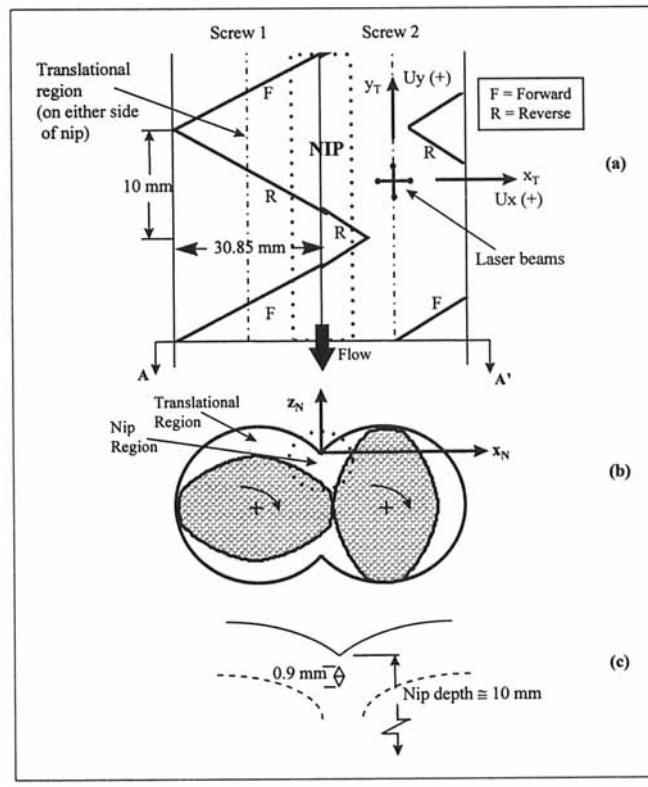

Figure 3. Measurement geometry: (a) top view through the Plexiglas window; (b) section A-A′ taken normal to the axes of the screws showing screw lobes at an encoder position of 0°; (c) relative size of the measurement volume.

screw axes. The beams intersect at an angle of 18° and form an elongated ellipsoidal measurement volume of approximately 0.9 mm × 0.1 mm × 0.1 mm. The orientation of the measurement volume and its relative size with respect to the nip dimension is shown in Figure 3c. The maximum dimension of the measurement volume is along the bisector of the four beams. During measurements, the probe was initially positioned so that the four beams focused on top of the screw flight tip, defined as $z_T = 0$. Velocity measurements were carried out at positions 0.2 mm apart along the negative z_T axis until the screw root was reached ($z_T = -4.8$ mm). Also shown in Figure 3b are the details of the nip region. Velocity data were obtained at a fixed position 0.5 mm directly below the nip ($z_N = -0.5$ mm).

Encoder

In order to keep track of the angular position of the screw shaft, an encoder (Servo-Tek Products, Hawthorne, NJ) was used (Karwe and Sernas, 1995, 1996). The encoder was fitted on the back end of the left screw shaft and interfaced with FVA of the LDA system. The encoder gives a pulse of 2.5 VDC for every 0.72° of rotation of the screw and a 5 VDC reset pulse after one full revolution, which is defined as 0° position of the encoder. Using this system, velocity data were obtained at discrete angular positions of the rotating screw shaft. A reference position of 0° was set arbitrarily when the

lobe of the forward-conveying screw immediately following the reverse element was vertical. Since the right and the left screw shaft have a phase difference of 90°, the orientation of one screw shaft automatically defines the orientation of the other screw shaft. Therefore, selection of zero position of the screw lobes does not affect the velocity measurements.

Correction factor for refraction

The laser beams bend due to refraction at the interface between air and the surface of the Plexiglas window, as shown in Figure 4. A correction factor must be applied to determine the actual location where the laser beams meet inside the screw channels, which is given as follows:

$$\text{Actual depth} \approx (\text{apparent depth}) \times \text{refractive index of Plexiglas,} \quad (1)$$

where apparent depth is the depth at which the laser beams would intersect in air. The error due to the approximation in Eq. 1 was estimated to be about 0.5% (Bakalis, 1996). Since the refractive index values of Plexiglas (1.507) and corn syrup (1.49) are very close to each other, the correction due to refraction at the interface between the two was negligibly small and was not applied to the collected data.

Results and Discussion

In the extrusion experiments, the two components of the velocity measured were tangential component, U_x, and the axial component, U_y, as shown in Figure 3a. Measurements were made at a given radial location within the screw channel. The probe is held in a fixed position relative to the barrel. As the screw rotates, the relative position of the measurement location with respect to the screw flight changes continuously. As seen by an observer fixed to the barrel, the measurement volume appears to move axially across the channel as the screw rotates. Actually, velocity measurements are made in different parts of the channel at every instant for one revolution and repeated for subsequent revolutions. The velocity measurements are repeated every 180°, since it is a double-start screw. Results from the measurements made in the translational region are discussed first, followed by the results in the nip region.

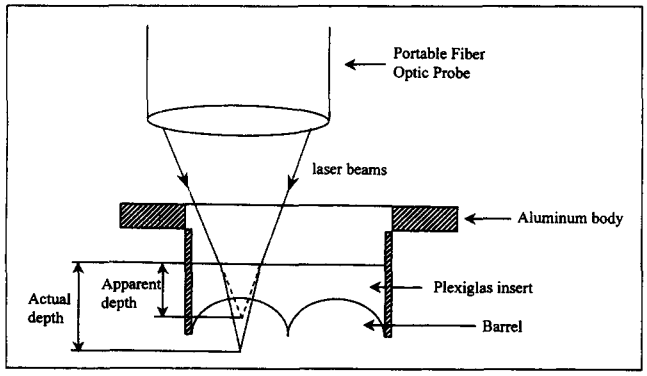

Figure 4. Actual and apparent depths where laser beams intersect due to refraction at the air–Plexiglas surface.

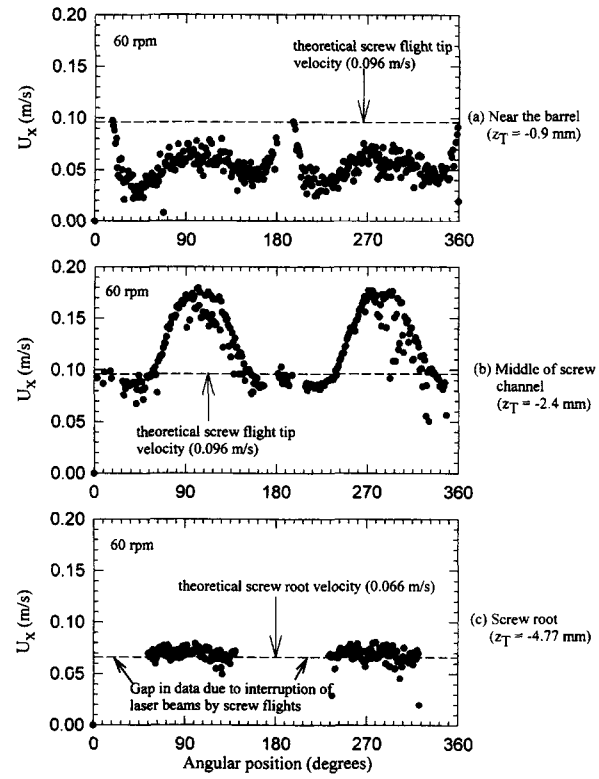

Figure 5. Variation of tangential velocity (U_x) with angular position of the screw shaft rotating at 60 rpm; mass flow rate of 21.5 kg/h at 27°C: (a) near the barrel; (b) middle of channel; (c) screw root.

Figures 5a, 5b, and 5c show the variation of the tangential velocity component U_x as a function of the angular position of the screw shaft for the screw speed of 60 rpm in the translational region. These measurements were made at distances of $z_T = -0.9$ mm (near the surface of the barrel), $z_T = -2.4$ mm (center of the channel, depthwise), and $z_T = -4.8$ mm (screw root) from the barrel surface, respectively. The axial position in which these measurements were made was the center of the reverse element. A gap in velocity data, corresponding to interruption of the laser beams by screw flights can be seen in Figures 5a–5c.

A closer examination of Figure 5a shows that maximum velocity occurred near the tip of the screw flight. This measured maximum velocity close to the barrel surface ($z_T = -0.9$ mm) agrees with theoretical velocity of the screw flight tip rotating at 60 rpm (0.096 m/s). Unlike the results of the forward-conveying element (Karwe and Sernas, 1996), where the U_x decreased continuously toward the middle of the screw channel, the U_x has a local maximum at the center of the screw channel near the encoder angles of 90° and 270°.

Figure 5b shows the tangential velocity component at the second measurement position, midway between the barrel and screw root ($z_T = -2.4$ mm). Tangential velocities of 0.18 m/s, which are higher than the calculated screw flight tip velocity of 0.096 m/s, were observed in the center of the channel (near encoder angle of 90° and 270°). These higher velocities are due to pressure flow. The drag flow component of a reverse-

conveying element is toward the hopper. However, the material has to move toward the die because the net flow is toward the die. This is achieved by the negative pressure gradient in the reverse element, that is, the pressure decreases along the downstream direction toward the die. It can be shown from simple analysis (Tayeb et al., 1988a) that the main component of flow in a reverse element is the pressure flow.

The two symmetric humps seen in Figure 5b are the velocities measured in each screw channel as explained earlier. No negative velocities were observed. As one moves away from the barrel toward the screw root, the flight thickness increases. This increases the gap in the data caused by the interruption of laser beams by screw flights.

The measured tangential velocity at the screw root, shown in Figure 5c, is very close to the theoretical screw-root velocity (0.066 m/s at 60 rpm). This also implies that there is no slippage between the fluid and the wall at the screw root for this material. There is no noticeable variation of the tangential velocity with angular position at the screw root due to the no-slip condition. This is also due to the fact that there is a wide region of constant screw radius near the screw root.

The variation of axial velocities along the angular position in the translational region are shown in Figures 6a, 6b, and 6c at $z_T = -0.9$ mm, $z_T = -2.4$ mm, and $z_T = -4.8$ mm, respectively. Again, the gaps in the data due to the interruption of the laser beam by the flights are evident. Based on the coordinate system shown in Figure 3a, the negative axial velocities imply flow toward the die. Note that the velocity scale in Figure 6 is expanded by a factor of 2 as compared to that in Figure 5. Small but finite axial velocities toward the die were observed near the barrel surface ($z_T = -0.9$ mm) as shown in Figure 6a. The variation of axial velocity along the angular position is minimal, although some asymmetry is observed. The reasons for this asymmetry are not yet known and are being investigated.

Figure 6b shows the axial velocities in the tangential region in the midpoint between the barrel surface and the screw root ($z_T = -2.4$ mm). Relatively high axial velocities of -0.03 m/s were observed in the middle of each screw channel (near encoder angles of 90° and 270°). These high axial velocities are due to the pressure flow in a reverse-conveying screw element as explained before. Figure 6c shows the axial velocity at the screw root ($z_T = -4.8$ mm). The measured axial velocity is close to zero at the screw root, as the screw rotates only along the x-direction and hence has no axial velocity component. Again, there does not seem to be any measurable slip at the screw root for this material.

Experiments were performed at different channel depths, from $z_T = 0$ mm (top of flight), in steps of 0.2 mm, to $z_T = -4.8$ mm (screw root), in the translational region. The tangential and axial velocities, similar to those illustrated in Figures 5 and 6, were obtained at each z_T position. The tangential and axial velocities at each z_T position in the middle of the channel for the reverse element were extracted from the data. The middle of the channel occurs at an encoder angular position of 90° in the reverse element. This follows from setting of the encoder at 0° on the screw flight and screw geometry. Figures 7a and 7b show extracted tangential- and

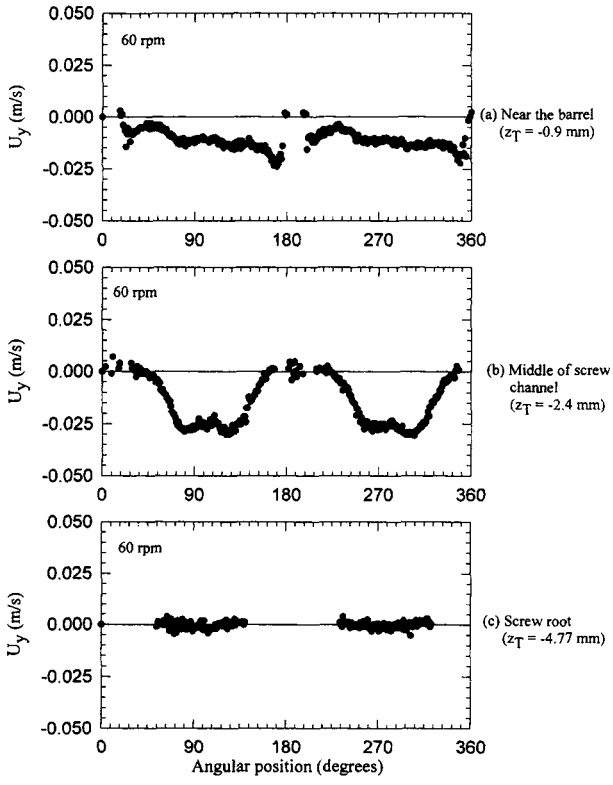

Figure 6. Variation of axial velocity (U_y) with angular position of the screw shaft rotating at 60 rpm; mass flow rate of 21.5 kg/h at 27°C: (a) near the barrel; (b) middle of channel; (c) screw root.

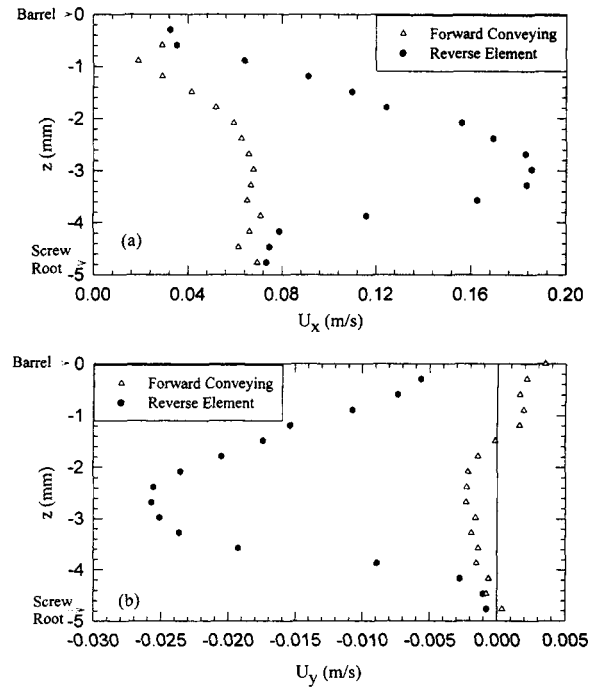

Figure 7. Variation of tangential and axial velocities with channel depth in the middle of the channel at a screw speed of 60 rpm; mass flow rate of 21.5 kg/h, at 27°C: (a) tangential velocity (U_x); (b) axial velocity (U_y).

axial-velocity profiles, respectively, from top of flight ($z_T = 0$ mm) to screw root ($z_T = -4.8$ mm) at this fixed angular position. Also shown in Figures 7a and 7b are depthwise variation of the tangential and axial velocities in the middle of the screw channel for the 20/10 forward-conveying element immediately following the reverse-conveying element. In this case, the middle of the channel occurred at an encoder angular position of 180°.

As seen in Figure 7a, small tangential velocities were observed close to the surface of the barrel in the reverse element. The highest velocity occurred below the midpoint of the space between the barrel and screw root, at $z_T \approx -3.0$ mm. In the forward-conveying element immediately following the reverse element, tangential velocities were much lower in magnitude. Near the screw root, the measured tangential velocity is close to the calculated screw root velocity (0.066 m/s) in both types of elements, suggesting that the no-slip condition exists there.

Figure 7b shows the variation of axial velocity in the translational region at various depths, from $z_T = -0$ mm to $z_T = -4.8$ mm in the center of the channel. As explained before, the center of the channel occurs at an encoder angular position of 90° for the reverse element and 180° in the forward-conveying element. Axial velocities in both reverse- and forward-conveying elements are zero at the screw root. The axial velocity in the channel of a reverse element is highest in magnitude in the middle due to pressure flow. The sharp gradients of velocity near the screw root and near the barrel impart high average shear rates to the material. Much lower axial velocities are observed in the channel of a forward-conveying element. In all of the measurements done in the translational region, positive values of axial velocity were not seen, implying no reversal of flow in the translational region, even for reverse-conveying screw elements.

Conventionally, in mathematical modeling of single-screw extrusion processes, the helical screw channel is unwound and treated as a long and shallow channel (Karwe and Jalura, 1990). The coordinate system is fixed to the screw root with the screw treated as stationary and the barrel moving in a direction opposite to the screw rotation. Furthermore, the coordinate system used is along this narrow channel, with the velocity components resolved in down-channel and cross-channel components. In this "barrel-moving" formulation, the measured axial U_x and tangential U_y velocities that can be transformed into down-channel (U_d) and cross-channel (U_n) components are as follows:

Forward conveying element

$$U_d = -U_x \cos\theta - U_y \sin\theta + \pi DN \cos\theta \tag{2}$$

$$U_n = U_x \sin\theta - U_y \cos\theta - \pi DN \sin\theta \tag{3}$$

Reverse element:

$$U_d = U_x \cos\theta - U_y \sin\theta - \pi DN \cos\theta \tag{4}$$

$$U_n = U_x \sin\theta + U_y \cos\theta - \pi DN \sin\theta, \tag{5}$$

where, θ is the helix angle, D is the screw-root diameter, and N is the number of revolutions of the screw per second. Different transformations have to be done for forward and reverse elements, as the down-channel and cross-channel coordinate axes are oriented differently, as shown in Figure 8. The down-channel (i) and cross-channel (ii) velocities in the barrel moving formulation in 20-mm-pitch forward and reverse elements are shown in Figures 8a and 8b, respectively. The velocity profiles are similar to those expected from theoretical considerations. The velocities at the screw root are zero, as the screw root is stationary.

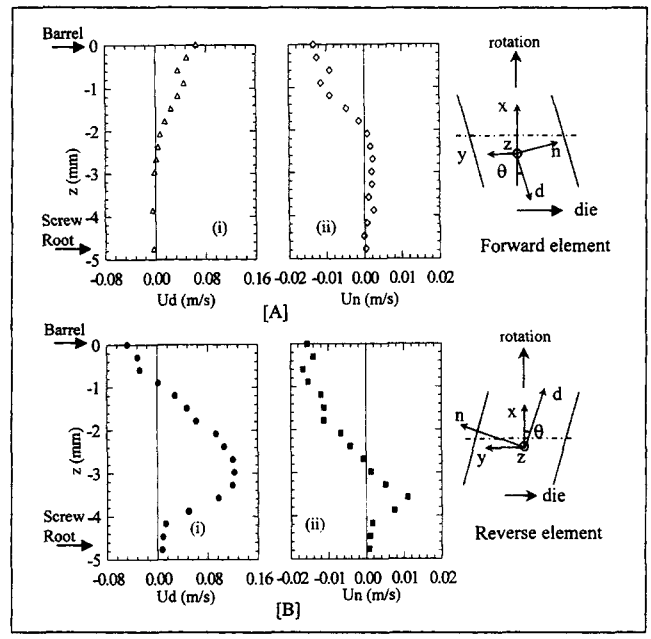

Figure 8. Down channel (i) and cross channel (ii) velocity profiles in the barrel-moving formulation in the translational region of forward [A] and reverse [B] elements at a screw speed of 60 rpm.

Velocities were measured in heavy corn syrup flowing at 21.5 kg/h at 27°C. These profiles were obtained by transformation of axial and tangential velocity data.

Figure 9 shows tangential and axial velocities measured in the intermeshing region (nip region). These measurements were made at $z_N = -0.5$ mm below the nip. The data are periodic; repeating every 180°, as the screw is a double-start screw with two channels. Again, gaps in the data appear where the screw flights cut the laser beams. In Figure 9a, high values of tangential velocity are observed near encoder angles of 90° and 270° (middle of the two channels of the reverse element), due to pressure flow. There are two velocity peaks at encoder angles just after 0° and 180° of 0.18 m/s. A closer look at the screw geometry shows that these are leakage flows that occur in the small clearances between the screw flights. This leakage flow is the result of pressure difference between the channels whose flights meet at the nip. The leakage flow occurs from a channel in one screw to a channel in the other screw. Since the U_x velocity is positive and the U_y velocity component is negative around 180°, the resultant direction of this leakage flow is toward the die. This occurs because pressure drop is toward the die in a reverse element. This is exactly the opposite to what was observed by Karwe and Sernas (1995) for a 28-mm forward-conveying element, where it was observed that the leakage flow was toward the hopper be-

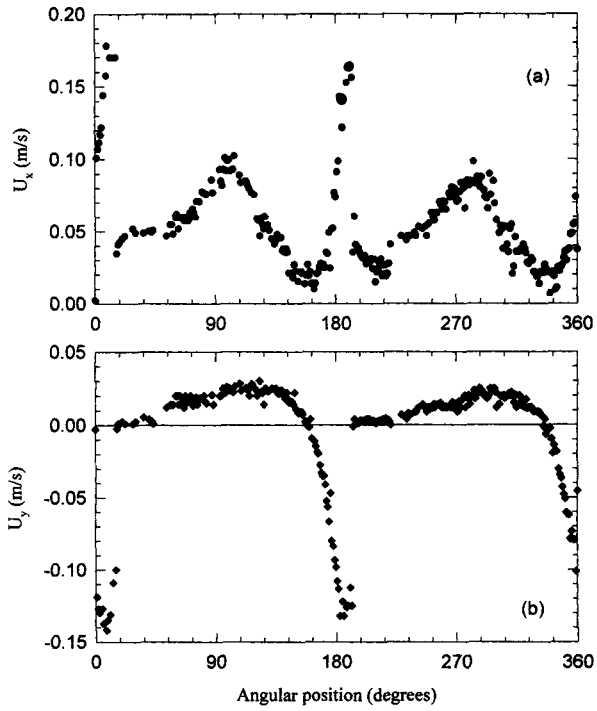

Figure 9. (a) Tangential (U_x) and (b) axial (U_y) velocities at a point 0.5 mm below the nip at screw speed of 60 rpm and mass flow rate of 21.5 kg/h at 27°C.

cause of increased pressure toward the die (Karwe and Sernas, 1995).

Axial velocities, shown in Figure 9b, are positive over a large region. Based on the coordinate system shown in Figure 3a, positive axial velocity is an indication of backflow (flow toward the hopper end of the extruder). Therefore, there is a significant backflow in the center of the reverse element in the nip area. As shown earlier, this effect is not observed in areas far away from the nip, that is, in the translational region. At the proximity of the screw flights (175° and 355°), the axial velocity drops to zero, as the rotating screw flights have no axial velocity.

The velocity profiles in the nip region show that the "jog" flow (Karwe and Sernas, 1995) in the reverse element is toward the hopper, unlike that of a forward-conveying element. The backflow occurs only in the nip region of the reverse element, and this contributes to an increase in the residence time. Further experiments are being performed to map the flow profiles in the vicinity of the nip region to determine over what domain of the intermeshing region the backflow occurs. This information is important for the development of mathematical models for each region, as suggested by Satrohartono et al. (1992).

Conclusion

Velocity profiles in a pilot-scale twin-screw extruder equipped with a Plexiglas window were mapped using a two-dimensional laser Doppler anemometry system. Tangential and axial velocities were measured in the translational and intermeshing (nip) region in the corn syrup at the center of a 20-mm-pitch reverse-conveying screw element. In the translational region, highest tangential and axial velocities were observed in the middle of the screw channel of the reverse element. Tangential velocity values were higher in the middle of the screw than the screw flight tip velocity. In the nip region, high tangential velocities associated with leakage flow in the gap between screw flights were observed. Positive axial velocities, indicating backflow (toward the hopper) were observed in the middle of the screw channel. No backflow was observed in the translational region.

Acknowledgments

This material is based upon work supported by the Cooperative State Research, Education, and Extension Service, U. S. Department of Agriculture, under Agreement No. 93-37500-2021. The authors acknowledge the equipment support provided by The Center of Advanced Food Technology, Rutgers University, for this study. The authors also thank Mr. Serafim Bakalis for useful suggestions.

Literature Cited

Bakalis, S., "Measurement of Velocity Distributions in the Screw Channels of a Co-rotating Twin-Screw Extruder," MS Thesis, Dept. of Food Science, Rutgers University, New Brunswick, NJ (1996).

Bigio, D., and S. Zerafati, "Numerical Procedure for Evaluation of Mixing in the Nip Region of Non-intermeshing Counter-rotating Twin-Screw Extruder," *SPE ANTEC Tech. Papers*, **34**, 85 (1988).

Booy, M. L., "Isothermal Flow of Viscous Liquids in Co-rotating Twin-Screw Devices," *Poly. Eng. Sci.*, **20**(18), 1220 (1980).

Chiruvella, R. V., Y. Jaluria, and A. H. Abib, "Numerical Simulation of Fluid Flow and Heat Transfer in a Single-Screw Extruder with Different Dies," *Poly. Eng. Sci.*, **35**, 261 (1995).

Colonna, P., J. P. Melcion, B. Vergnes, and C. Mercier, "Flow, Mixing, and Residence Time Distribution of Maize Starch within a Twin-Screw Extruder with a Longitudinally-split Barrel," *J. Cereal Sci.*, **1**, 115 (1983).

Choo, K. P., N. R. Neelakantan, and J. F. T. Pittman, "Experimental Deep Channel Velocity Profiles and Operating Characteristics for a Single-Screw Extruder," *Poly. Eng. Sci.*, **20**(5), 349 (1980).

Della Valle, G., J. Tayeb, and J. P. Melcion, "Relationship Between Extrusion Variables and Pressure and Temperature during Twin-Screw Extrusion Cooking of Starch," *J. Food Eng.*, **6**(6), 423 (1987).

Durst, F., A. Melling, and J. H. Whitelaw, *Principles and Practices of Laser Doppler Anemometry*, Academic Press, New York (1981).

Eccher, S., and A. Valentinotti, "Experimental Determination of Velocity Profiles in an Extruder Screw," *Ind. Eng. Chem.*, **50**(5), 829 (1958).

Fenner, R. T., *Principles of Polymer Processing*, Chemical Publishing, New York (1980).

Fletcher, S. I., T. J. Mac Master, P. Richmond, and A. C. Smith, "Physical and Rheological Assessment of Extrusion in Cooked Maize," *Thermal Processing and Quality of Food*, P. Zeuthen, ed., Elsevier, London, p. 233 (1984).

Harper, J. M., *Extrusion of Foods*, Vol. 1, CRC Press, Boca Raton, FL (1981).

Harper, J. M., "Food Extruders and Their Applications," *Extrusion Cooking*, C. Mercier, P. Linko, and J. M. Harper, eds., American Association of Cereal Chemists, St. Paul, MN, p. 1 (1989).

Karwe, M. V., and Y. Jaluria, "Numerical Simulation of Fluid Flow and Heat Transfer in a Single-Screw Extruder for Non-Newtonian Materials," *Numer. Heat Transfer*, **17** (Part A), 167 (1990).

Karwe, M. V., and V. Sernas, "Velocity Measurements in the Nip Region of a Co-rotating Twin-Screw Extruder Using Laser Doppler Anemometry," *SPE ANTEC*, **1**, 150 (1995).

Karwe, M. V., and V. Sernas, "Application of Laser Doppler Anemometry to Measure Velocity Distribution Inside the Screw Channel of a Twin-Screw Extruder," *J. Food Process Eng.*, **19**, 135 (1996).

Kiani, A., R. Rakos, and K. Sebastian, "Three-dimensional Computational Analysis of Fluted Mixing Devices," *SPE ANTEC Tech. Papers*, **35**, 62 (1989).

Kokini, J. L., C-T. Ho, and M. V. Karwe, eds., *Food Extrusion Science and Technology*, Dekker, New York (1992).
Kulashreshtha, M. K., C. A. Zaror, D. J. Jukes, and D. L. Pyle, "A Generalized Steady State Model for Twin-Screw Extruders," *Trans. Inst. Chem. Eng.*, **69**(C), 189 (1991).
Lai-Fook, R. A., A. Senouci, A. C. Smith, and D. P. Isherwood, "Pumping Characteristics of Self-wiping Twin-Screw Extruders—A Theoretical and Experimental Study on Biopolymer Extrusion," *Poly. Eng. Sci.*, **29**(7), 433 (1989).
McCarthy, K. L., R. J. Kauten, and C. K. Agemura, "Application of NMR Imaging to the Study of Velocity Profiles during Extrusion Processing," *Trends Food Sci. Technol.*, **3**, 167 (1992).
Mercier, C., P. Linko, and J. M. Harper, *Extrusion Cooking*, American Association of Cereal Chemists, St. Paul, MN (1989).
Mohr, W. D., J. B. Clapp, and F. C. Starr, "Flow Patterns in a Non-Newtonian Fluid in a Single-Screw Extruder," *SPE Trans.*, **113** (1961).
Rauwendaal, C., *Polymer Extrusion*, Hanser, New York (1990).
Sastrohartono, T., M. V. Karwe, and Y. Jaluria, "Numerical Simulation of Transport Phenomena in Co-rotating Twin-Screw Extruders for Non-Newtonian Fluids," *Num. Methods Ind. Form. Proc. NUMIFORM92*, J.-L Chenot, R. D. Wood, and O. C. Zienkiewitcz, eds., Balkema, Rotterdam, The Netherlands, p. 45 (1992).
Sastrohartono, T., M. V. Karwe, and Y. Jaluria, "Numerical Coupling of Multiple Region Simulations to Study Transport in a Twin-Screw Extruder," *Numer. Heat Transfer*, **25** (Part A), 541 (1994).
Sebastian, D. H., and R. Rokos, "Simulation of Transport Phenomena for Kneading Elements in Twin-Screw Extruders," *Food Extrusion Science and Technology*, J. L. Kokini, C-T. Ho, and M. V. Karwe, eds., Dekker, New York, p. 105 (1992).
Tadmor, Z., and C. G. Gogos, *Principles of Polymer Processing*, Wiley, New York (1979).
Tadmor, L., and I. Klein, *Engineering Principles of Plasticizing Extrusion*, Van-Nostrand-Reinhold, New York (1970).
Tayeb, J., Vergnes, B., and G. Della Valle, "Theoretical Computation of the Isothermal Flow Through the Reverse Screw Element of a Twin-Screw Extrusion Cooker," *J. Food Sci.*, **53**(2), 616 (1988a).
Tayeb, J., B. Vergnes, and G. Della Valle, "A Basic Model for a Twin-Screw Extruder," *J. Food Sci.*, **53**(4), 1047 (1988b).
Tayeb, J., G. Della Valle, C. Barnes, and B. Vergnes, "Simulation of Transport Phenomena in Twin-Screw Extruders," *Food Extrusion Science and Technology*, J. L. Kokini, C-T. Ho, and M. V. Karwe, eds., Dekker, New York, p. 41 (1992).
van Zuilichem, D. J., E. van Der Laan, W. Stolp and K. van't Riet, "Modeling of Heat Transfer in a Co-rotating Twin-Screw-Extruder," *Food Extrusion Science and Technology*, J. L. Kokini, C-T. Ho., and M. V. Karwe, eds., Dekker, New York, p. 149 (1992).
Wang, Y., and J. L. White, "Non-Newtonian Flow Modeling of Screw Regions of an Intermeshing Co-rotating Twin-Screw Extruder," *J. Non-Newtonian Fluid Mech.*, **32**, 19 (1989).
White, J. L., *Twin Screw Extrusion*, Hansen, New York (1991).
Yam, K. L., B. K. Gogoi, M. V. Karwe, and S. S. Wang, "Shear Conversion of Corn Meal by Reverse-Screw Elements during Twin-Screw Extrusion at Low Temperatures," *J. Food Sci.*, **59**(1), 113 (1994).

Manuscript received Oct. 24, 1996, and revision received July 3, 1997.